Pergamon

0017–9310(95)00374–6

Heat and mass transfer in wooden dowels during a simulated fire: an experimental and analytical study

J. A. MARDINI, A. S. LAVINE and V. K. DHIR

Mechanical and Aerospace Engineering Department, University of California, Los Angeles,
Los Angeles, CA 90095-1597, U.S.A.

Abstract—An experimental and analytical study of heat and mass transfer in wooden dowels during a simulated fire is presented in this paper. The goal of this study is to understand the processes of heat and mass transfer in wood during wildland fires. A mathematical model is developed to describe the processes of heating, drying and pyrolysis of wood until ignition occurs. The governing equations of the model consist of a set of mass conservation equations for each species present (wood, water, air and released hydrocarbons), a momentum equation (Darcy's Law), and an overall energy conservation equation. The equations of the model were solved numerically for the temperature, mass loss, moisture content, gas densities and pressure histories. The results of the mathematical model were verified experimentally using wooden dowels made of birch. The experiments were conducted in a specially designed wind tunnel equipped with radiant heating panels to simulate a fire flame. Air with a velocity of 2.2 m s^{-1}, simulating a typical wind during a real fire situation, was allowed to flow across the dowel. Time to ignition, temperature history and mass loss of the wooden dowels were measured in the experiments. A comparison between the experimental and analytical results showed good agreement. Copyright © 1996 Elsevier Science Ltd.

INTRODUCTION

The goal of this study is to understand the processes of heat and mass transfer in wood during wildland fires. An experimental and analytical study of heat and mass transfer in wooden dowels during a simulated fire is presented in this paper. Wooden dowels were used instead of green wood, which is involved in wildland fires, because of their documented properties and their nearly repeatable experimental results. The simulated fire is a plane wall made of high temperature radiant panels. A comparison between the results of the mathematical model and the experimental tests is presented.

When wood is exposed to a flame, the following physical processes occur: heating, drying, pyrolysis and ignition. All these processes are considered in the model developed here, except for ignition. The experiments were terminated when ignition at the surface of the dowel occurred.

Wood is composed of three phases, namely: a solid phase (called here the cell matrix), liquid phase (water) and gas phase (water vapor, air and other gases such as hydrocarbons). The three phases are interlinked in a random fashion that makes the modeling of the transfer processes difficult. Comstock [1] suggested modeling the wood as a series of rectangular ducts that are "taper ended and overlapping". The ducts are connected to each other by a series of small circular pits that allow the transmission of water from

one duct to another. Plumb *et al.* [2], Spolek and Plumb [3] and other researchers used Comstock's [1] model to develop correlations that were used in modeling wood drying. In order to develop a model that is valid at any location inside the wood, Plumb *et al.* [2] used the phase volume averaging technique among the three existing phases. The phase volume averaging method was used in this paper to derive the differential equations that govern the heat, mass and momentum transfer processes.

Pyrolysis is the process of thermal degradation of wood into gases (such as carbon dioxide and hydrocarbons) and tar. Pyrolysis starts when the temperature of wood reaches a certain threshold value which depends on the kind of wood, but is generally around 250°C. The rate at which wood loses mass due to pyrolysis increases rapidly with temperature. Kanury [4], Roberts [5] and Welker [6] suggested a first-order Arrhenius type equation for the pyrolysis process, while other researchers such as Lee *et al.* [7] suggested a second-order equation. The constants used in the Arrhenius model are the pyrolysis activation energy, E_p, and pre-exponential constant, K_p, whose values depend on the kind of wood. Kanury [4] and Roberts [5] suggested ranges for E_p and K_p to be used in the Arrhenius equation of pyrolysis. In this study, the values of the pyrolysis constants were chosen to be in the middle of those ranges. Since the pyrolysis process is a change of phase process, heat can be either absorbed or released. Lee *et al.* [7] sug-

NOMENCLATURE

A	area	ε_1	emissivity of dowel
C_p	specific heat	ε_2	emissivity of the heaters
D	diffusion coefficient of gases	ε_3	emissivity of the walls
D_{BT}	diffusion coefficient of bound water	ω	mass fraction
E_p	pyrolysis activation energy constant	ϕ	angular coordinate
F_{ij}	shape factor between surfaces i and j	μ	dynamic viscosity
FSP	fiber saturation point	ρ	density
H	convective heat transfer coefficient	σ	Stefan–Boltzmann constant.
h_{fg}	latent heat of vaporization of water		
h_p	heat of pyrolysis	Superscripts	
J	flux of bound water	i	intrinsic
k	conductivity	$\cdot$	time rate
K	permeability	$\overline{}$	average.
K_{mass}	convective mass transfer coefficient		
K_p	pyrolysis pre-exponential constant	Subscripts	
M	moisture content	1	water vapor
P	pressure	2	combustible gases
Q_r	radiant heat flux	3	air
r	radial coordinate	b	bound water
$\dot{r}$	rate of generation of mass	c	cell matrix
R_i	gas constant of species i	ch	char
R_0	radius of dowel	e	environment
R_u	universal gas constant	in	initial
t	time	r	radial
T	temperature	s	surface
V	velocity.	w	wood
		β	liquid
Greek symbols		γ	gas
ε	phase volume fraction	σ	solid.

gested that the pyrolysis process is exothermic, while Akita [8] and Klason [9] suggested that it is endothermic. In this paper, the pyrolysis process is considered to be endothermic.

Water exists inside the dowel in the form of liquid and vapor. A quantity called moisture content, M, is defined as a measure of the amount of both liquid and vapor water present. Moisture content is defined as the mass of water (liquid and vapor) divided by the mass of dry wood, expressed as a percentage. The liquid water inside the dowel could be either bound to the cell matrix of the wood or in the form of free water in the pores of the dowel. A quantity known as the fiber saturation point, FSP, is used as a criterion to determine whether the liquid water is bound or free. FSP is a threshold value of moisture content below which liquid water exists only as bound water inside the wood structure. In this paper, the moisture content is always less than the fiber saturation point.

Once heating of the dowel starts, liquid water leaves the wood to the outside in the form of water vapor (and possibly liquid depending upon the initial amount of water inside the wood) leading to its drying. The movement of water inside the wood is generally modeled as flow in a porous medium. For $M < FSP$,

the water is chemically bound to the structure of wood. A certain amount of energy is required to release this bound water from its site. The released bound water diffuses from one location to another, inside the wood, through the microvoids that exist inside the fuel element. Nelson [10, 11] suggested that the diffusion of bound water is due to the existence of a chemical potential gradient, while others suggested that it is due to the existence of a pressure gradient. Siau [12] developed a parametric model for the diffusion of bound water inside wood, whose coefficients are functions of the moisture and temperature gradients inside the wood. In this paper, the drying model used is based upon Siau's [12] study for the diffusion of bound water. At certain locations inside the microvoids, water is under saturation conditions. However, because of the phase volume averaging of the equations, the vapor pressure and temperature of water do not correspond to their saturation conditions. A correlation developed by Moyne [13] was used to account for the partial saturation of water.

Most of the existing fire models do not account for all the processes that affect the thermal response and mass loss of wood during fires. For example, Kung

[14] developed a model in which he neglected the moisture and dropped the resistance to the flow of gases inside the wood. This led to the assumption that all the released gases are available instantly at the surface of the wood. Fredlund [15] developed a model to study the processes of heat and mass transfer in timber structures during fires. In his model, Fredlund assumed that the liquid water evaporates at its location inside the wood. Thus, mass transfer occurs in the gas phase only. Other researchers studied fires in dry wood only, e.g. Kansa et al. [16]. Models of wood drying are also relevant to the present study. In order to maintain the integrity of the wood structure while the moisture is being removed, the heating rate of the wood is slow and the maximum temperature it is allowed to reach is in the neighborhood of 373 K (the normal boiling point of water). Thus the drying models exclude the pyrolysis process (which starts at temperatures that exceed 473 K) such as in Plumb et al. [2], Shusheng et al. [17] and Kiranoudis et al. [18].

In this paper a model is developed that accounts for water and gas movement, local evaporation of liquid water, and pyrolysis within the wood while it is exposed to a simulated fire flame. The effect of varying the governing parameters such as: the initial moisture content of the dowel, its size, its kind and the speed of air flowing over it will be investigated in a later paper.

PROBLEM STATEMENT

Figure 1(b) shows a dowel placed inside the testing site of the experimental set-up. The dowel is a cylindrical piece of birch of 25.4 mm diameter and 355 mm length. The dowel is placed vertically at a distance of 140 mm from an assembly of heaters, referred to here as a simulated fire flame, on top of a digital scale. The simulated fire flame emits energy at a surface temperature of 940 K, which is within the range of the temperature of a real fire flame. Air at a speed of 2.2 m s^{-1}, which is a representative wind speed in a fire situation, flows across the dowel. The goal of this paper is to develop an analytical model that predicts the temperature history and mass loss from the dowel while being exposed to the heaters. The results of the

Fig. 1. Experimental set-up and a dowel in the testing site.

model are to be verified experimentally using the set-up shown in Fig. 1(a).

THEORETICAL MODEL

The model consists of a set of equations that describes the heat and mass transfer within the dowel during its exposure to the heaters. The equations of the model are solved numerically for the temperature and the mass loss of the dowel. In order to be able to compare the theoretical and experimental results under similar conditions, quantities measured in the experiments such as: the temperature histories of the heaters, walls of the test section, and air blowing across the dowel were used wherever they appear in the model.

The following is a list of the assumptions used in developing the mathematical model:

(1) porosity of wood is uniform;
(2) structural stability of wood is preserved;
(3) phase volume averaging is used to develop the conservation equations, Whitaker [19];
(4) local thermal equilibrium exists among the three phases within the wood at any time and any location;
(5) axial variation is negligible, thus a two-dimensional (r, ϕ) model is used;
(6) unsaturated conditions between liquid water and its vapor are accounted for by the use of Moyne's [13] correlation;
(7) pyrolysis of wood is modeled with a first-order Arrhenius equation;
(8) Darcy's law is used to calculate the bulk velocity of the gases, $\mathbf{V}_\gamma$;
(9) diffusion coefficients of all gases are equal;
(10) enthalpy exchange due to species inter-diffusion is ignored;
(11) all gases are ideal with constant specific heats;
(12) the gases in the environment are transparent;
(13) emissivities of the simulated fire flame and the dowel are constant;
(14) three body radiation network between the dowel, heaters and the walls of the wind tunnel is assumed;
(15) for radiation exchange, the surfaces are modeled as gray and diffuse;
(16) Newton's cooling law is used to model the heat and mass convection from the surface of the dowel; the convective heat transfer coefficient is determined from published experimental results by Krall [20]; and heat and mass transfer analogy is used to determine the convective mass transfer coefficient;
(17) the mass transfer of the species from the surface of the dowel was calculated using the low mass transfer rate theory. The result of this theory was compared to that of the high mass transfer rate theory, according to Mills [21], and was found to be acceptable for this problem because the mass fractions of the species involved were small.

These assumptions are discussed further and jus-
tified in Mardini [22]. With these assumptions the
governing equations, whose derivation can be found
in detail in Mardini [22], are as follows:

Conservation of mass of water vapor

$$\frac{\partial}{\partial t}(\varepsilon_\gamma \rho_{\gamma 1}^i) + \nabla \cdot (\varepsilon_\gamma \rho_{\gamma 1}^i \mathbf{V}_\gamma) = \nabla \cdot (\varepsilon_\gamma D \nabla \rho_{\gamma 1}^i) + \dot{r}_{\gamma 1}. \quad (1)$$

Conservation of mass of bound water

$$\frac{\partial}{\partial t}(\varepsilon_\sigma \rho_b^i) + \nabla \cdot \mathbf{J} = -\dot{r}_{\gamma 1}. \quad (2)$$

$\mathbf{J}$ is the flux of bound liquid water which is expressed
as follows, Siau [12]:

$$\mathbf{J} = -\frac{\rho_\sigma D_{\mathrm{BT}} M}{100(R_u T + 70M)}\left\{\frac{(9200 - 70M)}{T}\nabla T\right.$$

$$\left. + \frac{R_u T + 70M}{M}\nabla M\right\}. \quad (3)$$

In equation (3), D_{BT} is the diffusion coefficient of
bound liquid water within the cell matrix and is ex-
pressed as follows, Siau [12]:

$$D_{\mathrm{BT}} = 7 \times 10^{-6}\exp\left\{-\frac{9200 - 70M}{R_u T}\right\} \ (\mathrm{m^2\,s^{-1}}).$$

$$(4)$$

In equations (3) and (4), T is in K and the rest of
the variables are in SI units. Adding equations (1) and
(2) and defining $M = (\varepsilon_\sigma \rho_b^i + \varepsilon_\gamma \rho_{\gamma 1}^i)/\rho_\sigma \times 100$, the
moisture content equation is

$$\frac{\partial M}{\partial t} + \frac{100}{\rho_\sigma}\nabla \cdot (\varepsilon_\gamma \rho_{\gamma 1}^i \mathbf{V}_\gamma) =$$

$$\nabla \cdot \left\{D_{\mathrm{BT}}\left[\left(\frac{M(9200 - 70M)}{T(R_u T + 70M)}\right)\nabla T + \nabla M\right]\right\}$$

$$+ \frac{100}{\rho_\sigma}\nabla \cdot (\varepsilon_\gamma D \nabla \rho_{\gamma 1}^i) \quad (5)$$

where ε_γ and ε_σ are the volume fractions of the gas and
solid phases in wood, respectively. The values of ε_γ
and ε_σ are evaluated using correlations derived by Siau
[12] and are found to be 0.449 and 0.551, respectively.

Conservation of mass of combustible gases

$$\frac{\partial}{\partial t}(\varepsilon_\gamma \rho_{\gamma 2}^i) + \nabla \cdot (\varepsilon_\gamma \rho_{\gamma 2}^i \mathbf{V}_\gamma) = \nabla \cdot (\varepsilon_\gamma D \nabla \rho_{\gamma 2}^i) + \dot{r}_\sigma. \quad (6)$$

Conservation of mass of air

$$\frac{\partial}{\partial t}(\varepsilon_\gamma \rho_{\gamma 3}^i) + \nabla \cdot (\varepsilon_\gamma \rho_{\gamma 3}^i \mathbf{V}_\gamma) = \nabla \cdot (\varepsilon_\gamma D \nabla \rho_{\gamma 3}^i). \quad (7)$$

In the above equations, D is the diffusion coefficient
of gases inside wood and is expressed as follows,
Stamm [23]:

$$D = 6 \times 10^{-6}\left(\frac{P_{\mathrm{ref}}}{P_\gamma^i}\right)\left(\frac{T}{T_{\mathrm{ref}}}\right)^{1.75} (\mathrm{m^2\,s^{-1}}) \quad (8)$$

where P_{ref} and T_{ref} are reference pressure ($=101\,300$
Pa) and reference temperature ($=273$ K), respec-
tively.

Conservation of mass of wood

$$\frac{\partial \rho_c^i}{\partial t} = -\dot{r}_\sigma = -K_p(\rho_c^i - \rho_{\mathrm{ch}})\exp\left(-\frac{E_p}{R_u T}\right). \quad (9)$$

Ideal gas law

$$P_{\gamma j} = \rho_{\gamma j} R_j T \quad (10)$$

where $j = 1, 2$ or 3. In order to account for the partial
saturation that exists between liquid water and its
vapor, an empirical correlation obtained by Moyne
[13] is used. Moyne's [13] correlation is

$$P_{\gamma 1} = P_{\gamma 1,s}\exp\{(17.884 - 0.1423T$$

$$+ 2.36 \times 10^{-4}T^2)(1.0327 - 6.74 \times 10^{-4}T)^{0.92M}\}. \quad (11)$$

$P_{\gamma 1,s}$ is the saturated partial pressure of water vapor
in Pa and T is the local temperature in K.

Total gas density

$$\rho_\gamma = \rho_{\gamma 1} + \rho_{\gamma 2} + \rho_{\gamma 3}. \quad (12)$$

Total gas pressure

$$P_\gamma = P_{\gamma 1} + P_{\gamma 2} + P_{\gamma 3}. \quad (13)$$

Gas bulk velocity ($\mathbf{V}_\gamma$)

$$\mathbf{V}_\gamma = -\frac{K_\gamma}{\mu_\gamma}\nabla P_\gamma. \quad (14)$$

In the above equations, the intrinsic quantities (with
superscript i) and extrinsic quantities (without any
superscript) are related by their corresponding phase
volume fraction. For example, the intrinsic density of
water vapor is correlated to its extrinsic counterpart
as follows:

$$\varepsilon_\gamma = \frac{\rho_{\gamma 1}}{\rho_{\gamma 1}^i}. \quad (15)$$

Energy equation

$$\frac{\partial}{\partial t}(\overline{\rho C_p}T) + \nabla \cdot \left(\sum_{j=1}^{3}\varepsilon_\gamma \rho_{\gamma j}^i C_{pi}\mathbf{V}_\gamma T\right)$$

$$= \nabla \cdot (\bar{k}\nabla T) - \dot{r}_{\gamma 1}h_{\mathrm{fg}} - \dot{r}_\sigma h_p \quad (16)$$

$$\overline{\rho C_p} = \varepsilon_\sigma(\rho^i C_p)_c + (\rho C_p)_M + \varepsilon_\gamma(\rho C_p)_\gamma \quad (17)$$

$$\bar{k} = k_w + \varepsilon_\gamma(\omega_2 k_{\gamma 2} + \omega_3 k_{\gamma 3}) \quad (18)$$

$$\omega_j = \frac{\rho_{\gamma j}}{\rho_\gamma}. \quad (19)$$

Here $(\rho^i C_p)_c$ is the heat capacitance of the cell matrix
of wood given by Siau [12]: $(\rho^i C_p)_c = \rho_c^i$
$(1120 + 4.595T)$, where T is in $^\circ$C and $(\rho^i C_p)_c$ is in SI
units. The quantity $(\rho C_p)_M$ is the heat capacitance of

the moisture content inside the dowel and is defined as: $(\rho C_p)_M = \rho_\sigma C_{p\beta} M/100$. The quantity $(\rho C_p)_\gamma$ is the heat capacitance of the mixture of air and released volatiles and is defined as $(\rho C_p)_\gamma = \rho_{\gamma2}^i C_{p\gamma2} + \rho_{\gamma3}^i C_{p\gamma3}$. The quantity k_w is the conductivity of the cell matrix and moisture content combined and is given by Siau [12] as: $k_w = (\rho_\sigma/1000)(0.201 + 0.0038M) + 0.0239$, where ρ_σ is the extrinsic density of dry wood in kg m^{-3}, which is obtained by measuring the mass of the dowel and dividing it by its volume, and k_w is in SI units. The quantity h_{fg} is the latent heat of vaporization of bound water, which includes the energy required to release the bound water from the structure of the wood, in addition to the energy required for vaporization. In the model, h_{fg} is taken to depend on moisture content, according to the measurements of Skaar and Siau [24].

In the above equations, ∇ is the divergence in cylindrical coordinates.

Initial and boundary conditions

Initially the temperature and all the species concentrations, except for the moisture content, are assumed uniform throughout the dowel and equal to those outside in the environment. The environment temperature, and mass fractions of water vapor, air and volatiles are 300 K, 0.0092, 0.9908 and 0.0, respectively. The moisture content is assumed to be uniform within the dowel, equal to its initial value M_{in}, except at the surface where it is assumed to be equal to that present in the environment, $M = 0.05\%$.

Radial boundary condition. At $r = 0$ all variables, i.e. $\rho_{\gamma1}^i$, $\rho_{\gamma2}^i$, $\rho_{\gamma3}^i$, T and M are finite.
At $r = R_0$, we have:
water (liquid + vapor)

$$J_r|_s + \rho_{\gamma1}^i V_{\gamma r} - D\frac{\partial\rho_{\gamma1}^i}{\partial r} = K_{mass}(\rho_{\gamma1}^i - \rho_{\gamma1,e}) \quad (20)$$

combustible volatiles

$$\rho_{\gamma2}^i V_{\gamma r} - D\frac{\partial\rho_{\gamma2}^i}{\partial r} = K_{mass}(\rho_{\gamma2}^i - \rho_{\gamma2,e}) \quad (21)$$

air

$$\rho_{\gamma3}^i V_{\gamma r} - D\frac{\partial\rho_{\gamma3}^i}{\partial r} = K_{mass}(\rho_{\gamma3}^i - \rho_{\gamma3,e}) \quad (22)$$

energy equation

$$-\bar{k}\frac{\partial T}{\partial r} = H(T - T_e) + \sum_{j=1}^{3}\varepsilon_j\rho_{\gamma j}^i V_{\gamma j}C_{p\gamma j}(T - T_e)$$
$$- Q_r + J_r|_s h_{fg}. \quad (23)$$

By conducting an order of magnitude analysis, it was found that the second term on the right hand side, enthalpy flux due to the gas phase, is small compared to the other terms. Thus, this term was not accounted for while performing the numerical calculations. H is the local convective heat transfer coefficient for flow

across a cylinder which is a function of the angular location. Values for H are obtained from the results of a study by Krall [20] for flow across heated cylinders. K_{mass} is the local mass transfer convective coefficient and it is obtained by using the analogy between heat and mass transfer. Q_r is the local net radiant heat flux reaching the dowel at its surface and is evaluated by solving the radiation equations for a three surface enclosure. The three surfaces are: the dowel, the heaters and the walls of the wind tunnel. An expression for the shape factor between a differential surface area of a cylinder (dowel) and a parallel plane surface (heaters) is as follows (Siegel and Howell [25]): $F_{12} = 1/2(1 + \cos\phi)$.

Angular boundary condition.

$$f|_{\phi=0} = f|_{\phi=2\pi} \quad (24)$$

$$\frac{\partial f}{\partial \phi}\Big|_{\phi=0} = \frac{\partial f}{\partial \phi}\Big|_{\phi=2\pi} \quad (25)$$

where f is any of the variables: $\rho_{\gamma1}^i$, $\rho_{\gamma2}^i$, $\rho_{\gamma3}^i$, T or M.

Table 1 shows the values of the parameters used in the model. These values were selected in the middle of the ranges suggested in the literature. The values of $C_{p\beta}$, $C_{p\gamma1}$, $C_{p\gamma2}$, $C_{p\gamma3}$, $k_{\gamma1}$, $k_{\gamma2}$, $k_{\gamma3}$, ρ_c and μ_γ were obtained from Mills [21]. The values of the pyrolysis constants E_p, h_p and K_p were obtained from Roberts [5]. The values of FSP and ρ_c^i were obtained from Siau [12]. The value of K_γ was obtained from Spolek and Plumb [3]. The values of ε_1 and ε_3 were obtained from Siegel and Howell [25]. The value of ρ_{ch} was obtained from Sussot [26]. The value of ε_2 was provided by the manufacturer of the heaters used in the wind tunnel. The values of the rest of the parameters were obtained by measurement.

A sensitivity analysis was conducted on several of the variables, including one which posed a particular concern: the fiber saturation point, *FSP*. *FSP* decreases linearly with increasing temperature (Siau [12]); however, a constant value of 30% was used here. A test was run in which a constant value of 10% was used, and the effect on the results was found to be negligible.

Table 1. Values of variables used in the model

Variable	Value	Variable	Value
$C_{p\beta}$	4.18 kJ kg^{-1} K^{-1}	K_γ	2×10^{-18} m^2
$C_{p\gamma1}$	1.90 kJ kg^{-1} K^{-1}	M_{in}	8%
$C_{p\gamma2}$	1.005 kJ kg^{-1} K^{-1}	T_e	300 K
$C_{p\gamma3}$	1.005 kJ kg^{-1} K^{-1}	ε_1	0.60
R_0	0.01270 m	ε_2	0.90
E_p	28 kcal mol^{-1} K^{-1}	ε_3	0.70
FSP	30%	μ_γ	2×10^{-7} kg m^{-1} s^{-1}
h_p	400 kJ kg^{-1}	ρ_c^i	1600 kg m^{-3}
K_p	6×10^7 s^{-1}	ρ_{ch}	180 kg m^{-3}
$k_{\gamma1}$	0.02 W m^{-1} K^{-1}	ρ_e	1.04 kg m^{-3}
$k_{\gamma2}$	0.03 W m^{-1} K^{-1}	ρ_σ	570 kg m^{-3}
$k_{\gamma2}$	0.03 W m^{-1} K^{-1}		

METHOD OF SOLUTION

A computer program was developed to solve equations (1)–(23) for all the unknowns including M, T, P, and the mass of the dowel. The differential equations were integrated in time using the trapezoidal rule. The spatial integration was performed over control volumes, as in Patankar [27]. Second-order centered differencing was used for the diffusion terms, and the upwind scheme was used for the convective terms to ensure stability. Because of the nonlinearity of the governing equations, the discretized equations were solved iteratively within a time step. A variable time step was used to accommodate the evaporation process. Initially, the time step was set to 10 s. The time step was then halved if the moisture content calculated was found to be negative. Negative moisture content is caused by over evaporation of water due to large time steps.

The computational domain consisted of 10 radial nodes and 30 angular nodes. It was found that by doubling the number of nodes in each direction, a maximum difference of 4.5°C in the subsurface temperature and a maximum difference of 3 mg (out of an initial mass of 86.7 grams) in the mass history were obtained.

A convergence test was performed on the time step by using a dry dowel, since in the case of a moist dowel a variable time step was used. It was found that by halving the time step from 10 s to 5 s, a maximum difference of 0.9°C in the subsurface temperature and a maximum difference of 0.9 mg in the mass of the dowel were observed.

Fig. 2. A dowel with embedded thermocouples.

EXPERIMENTAL APPARATUS AND PROCEDURE

In order to validate the results of the model, an experimental rig was built. The experimental set-up consisted of a wind tunnel of an overall length of 3.05 m and a cross-section of 33 × 24.1 cm. The testing site consisted of a trapezoid of 38.1 × 24.1 cm as shown in Fig. 1(a,b). One of the inclined sides of the trapezoid consisted of heating panels that deliver heat at a surface temperature of about 940 K. The temperature of the heaters were controlled by using variacs (to adjust the input power) and thermocouples installed at their surfaces. The wind tunnel was equipped with a centrifugal fan that can deliver air at a velocity up to 12.8 m s^{-1}. The experiment set-up was equipped with a digital scale that detects a mass change of ±0.01 grams. The scale was placed underneath the testing site and the dowel was placed on top of the weighing platform. The measured quantities in the experiment were the temperature, mass history and time to ignition of the dowel.

In the experiment, a cylindrical wooden dowel (made of birch) of 25.4 mm diameter and 355 mm length was placed at the center of the testing site. The dowel was instrumented with eight thermocouples (type K, 30 AWG) placed at different locations inside

the dowel as shown in Fig. 2. Six of the thermocouples were placed at a distance of approximately 1.1 mm, called here the subsurface, from the surface of the dowel facing the heaters, while the other two thermocouples were placed at the center of the dowel, but at different axial locations. From preliminary analytical studies it was found that under such conditions, ignition occurs at an angular location corresponding to $\phi = 40°$, see Fig. 1(b) for the definition of ϕ. Thus, two of the subsurface thermocouples were placed at $\phi = 40°$, but at different axial locations.

Before starting a test, the dowel was instrumented with the thermocouples outside the wind tunnel and then placed inside the testing site. The heaters were then turned on. It took about 2 min for the heaters to reach their steady state temperature of 940 K. Air at a velocity of 2.2 m s^{-1} was blown over the dowel. The temperature and the mass of the dowel were measured continuously until glowing ignition at its surface was visually observed.

The experimental results reported in this paper are the average of six tests conducted on birch dowels under similar conditions to ensure repeatability. There was an uncertainty in the locations (angular, axial and radial) of the thermocouples. This uncertainty
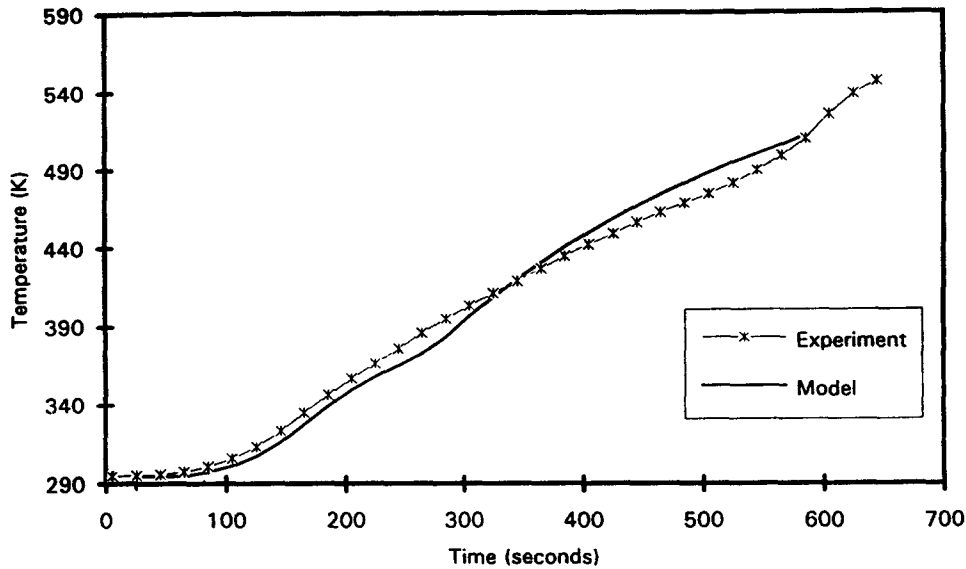
Fig. 3. Subsurface temperature history at $\phi = 40°$.

emanated from the visual alignment of the dowel inside the testing site and the size of the bead of the thermocouples. Because of this uncertainty and the differences among the different tests (due to the inherent differences in the dowels), the maximum standard deviation of the measured subsurface temperature at the same angular and axial location (where ignition occurred) is 40 K. The maximum difference between the two subsurface temperatures, measured at the same angular location (where ignition occurred), but at different axial locations (about 5 cm apart), was 15 K. Since this is less than the standard deviation, and also small compared with the temperature difference between the dowel and surrounding air (which reaches 225 K within 550 s of the start of testing), the assumption of two-dimensional modeling is valid.

RESULTS AND DISCUSSION

Figure 3 shows a comparison between the measured and predicted subsurface temperatures of the dowels at the location closest to where ignition first occurred. The measured temperature is the average of six experimental tests conducted on birch dowels under almost identical conditions. The temperature, obtained in the experiment, is the average of temperatures measured with the thermocouples labeled TC3 and TC7, Fig. 2. These thermocouples are located at approximately 1.1 mm from the surface of the dowel facing the heaters.

Figure 3 shows excellent agreement between the measured and the predicted temperatures. There is a small discrepancy when the temperature is close to 373 K, the saturation temperature of water at atmospheric pressure. Presumably, the drying model is not highly accurate. The rate of increase of subsurface temperature decreases with time because of the pyrolysis and evaporation processes which are both endo-

thermic, but the model slightly overpredicts this effect. In the experiments, released gases were visually observed to leave the dowel in the form of a gray cloud around 520 s after the test started. This cloud of gases is accompanied by a change in the heating rate of the dowel as shown by the measured temperature curve in Fig. 3. This change is likely due to the exothermic reaction between the released combustible gases and air. At this stage the exothermic reaction is not strong enough to cause ignition. At about 600 s, the dowel ignited causing a sharper rise in the measured temperature as shown in Fig. 3. This is caused by the heat released from the exothermic reaction between the released gases and air due to combustion. The model does not predict these slope increases because it does not account for the exothermic reaction. The ignition was observed as glowing on the surface of the dowel. The maximum temperature of the dowel at the instant of ignition was about 550 K. As seen in Fig. 3, the model predicts the temperature history with relatively good agreement with the experiment, except for the early stage of evaporation of water and during the time an exothermic reaction between the released gases and air takes place.

Figure 4 shows a comparison between the predicted and measured temperatures at the center of the dowel. A comparison between the model and the experiment shows reasonable agreement until around 400 s, when the measured temperature levels off and the model does not. The measured temperature leveled in the range between 368 and 384 K, which is near 373 K, the boiling temperature of water at atmospheric pressure. This leveling could be a result of the holes drilled in the wood to place the thermocouples, which might bring the pressure at these locations to atmospheric. Since the model assumed the structure of wood was intact, the predicted pressure was greater than atmospheric, corresponding to an increased saturation temperature.
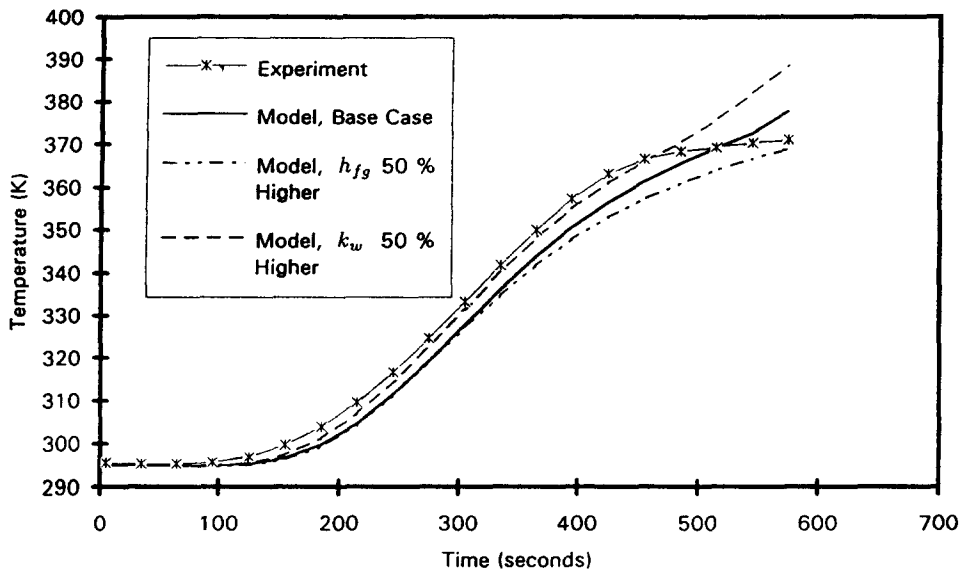
Fig. 4. Center temperature history and effects of h_{fg} and k_w.

Another possible explanation for the discrepancy could be the values used for various parameters in the model. The figure shows the effect of changes in two of the physical properties, the thermal conductivity of wood, k_w, and the latent heat of vaporization of bound water, h_{fg}. Increasing the conductivity of wood by 50% yields much better agreement between the predicted and measured center temperature. By increasing h_{fg} by 50%, the predicted temperature shows a slower rate of temperature increase and better agreement with the measurements in the later period. It is not known whether these higher values of k_w and h_{fg} are reasonable; however, it is known that the physical properties of wood are species dependent. For instance, in a paper by Nelson [11], the value of h_{fg} for Sitka spruce is about 15% higher than that used here for an unspecified type of wood (Skaar and Siau [24]). In a study by TenWolde *et al.* [28], under certain conditions the conductivity of wood can be 26% higher than the value used here.

Figure 5 shows a comparison between the predicted and measured subsurface temperatures at three different angular locations. The angular locations are: $\phi = -40°$, $0°$, $+40°$ [see Fig. 1(b) for definition of ϕ]. Each of the measured temperatures is the average of two axial locations (at the same angular location) over six different runs. The predicted temperatures are for locations that correspond to the measured angular ones. Radiation and convection are two competing modes of heat transfer in this problem. The radiation heat flux reaching the dowel is maximum at $\phi = 0°$. For the convection heat flux, the location of minimum heat loss for cross flow over a vertical cylinder depends on the air speed. For an air speed of 2.2 m s^{-1}, the minimum occurs at around $128°$ from the stagnation point [20] which corresponds to $\phi = 48°$. The location of maximum net heat flux varies with time, as the relative contributions of radiation and convection

change. At 550 s, the location of the maximum net heat flux is found (from the model) to be at $\phi = 40°$. Both the predicted and measured temperatures showed the same order in their values, i.e. the temperature is maximum at $\phi = 40°$ followed by that at $\phi = 0°$ and then at $\phi = -40°$. The agreement is reasonably good.

Figure 6 shows a comparison between the predicted and measured mass history of the dowel. The mass loss from the dowel is due to the migration of moisture from the dowel and to its pyrolysis. The mass loss measured in the experiment was a combination of both the moisture migration and the pyrolysis of the dowel. The measured mass history is the average of the six tests conducted.

Figure 6 shows two graphs for the predicted mass history: the solid line (base case) is when a convective boundary condition for the moisture content is used, as presented in this paper, and the dashed line is obtained when the moisture content at the surface of the dowel is specified to be equal to that of the surrounding. It is noticed that by using the convective boundary condition for the moisture content, the model underpredicts the rate of mass loss of the dowel during the first 300 s. The underprediction during this time period is apparently because the moisture movement model does not predict enough moisture leaving the dowel. One potential mechanism for increasing the rate at which moisture leaves the dowel is to increase the permeability. However, increasing the permeability by two orders of magnitude over its value in Table 1 resulted in a very small effect on the mass loss. Specifying the moisture content at the surface to be equal to the surrounding successfully increases the rate at which moisture leaves the dowel, and yields excellent agreement with the measured mass loss. This excellent agreement does not mean that this boundary condition is correct. It simply
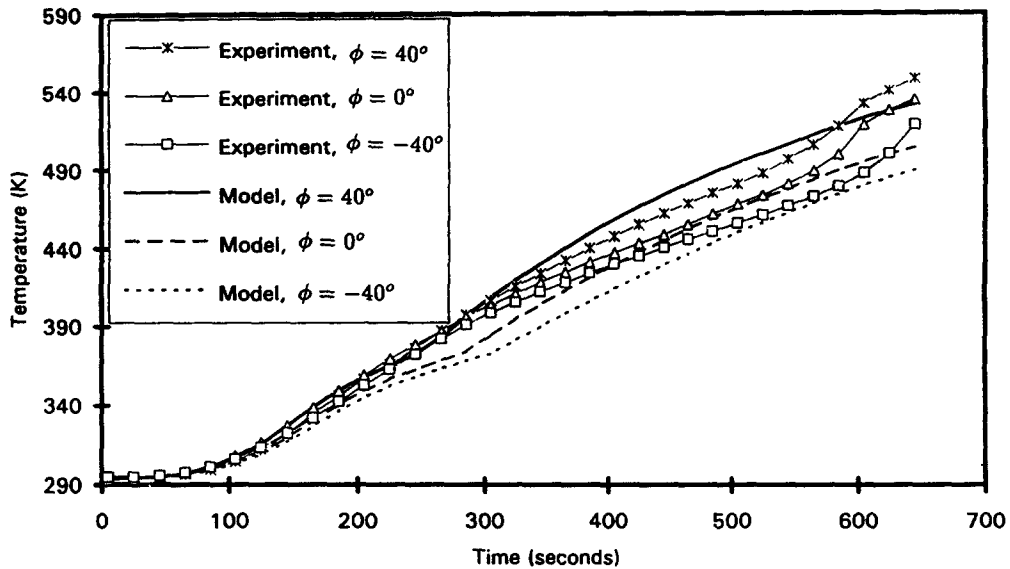
Fig. 5. Subsurface temperature at different angular locations.
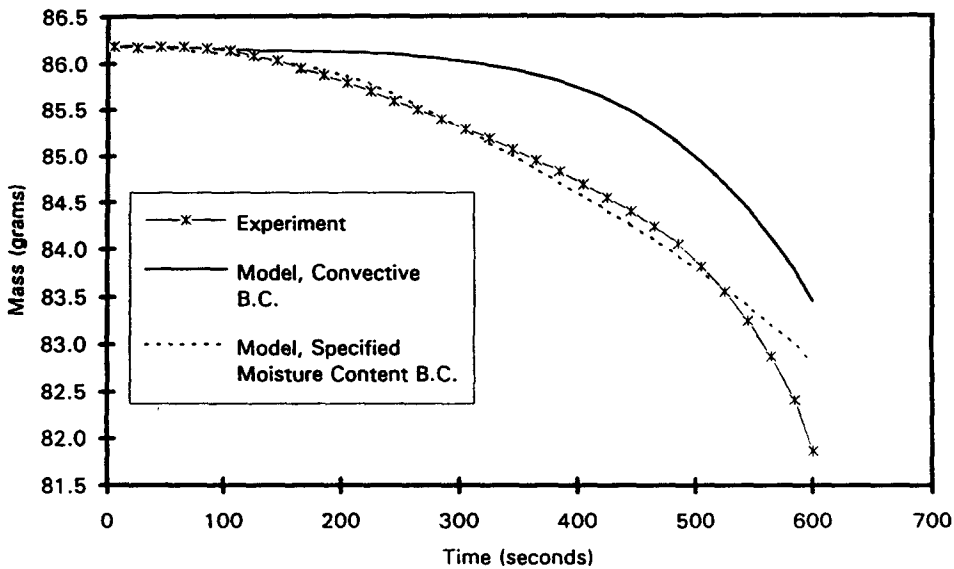
Fig. 6. Mass loss history.

underscores the fact that the amount of moisture leaving the dowel should be larger, and thus the model for moisture movement is in need of modification. The model used here is suitable for wood drying. In wood drying the wood is heated at a slow rate causing the temperature of wood to be almost uniform, and to remain in the vicinity of 100°C. However, this is not the case in fires, where large temperature gradients and higher temperatures occur as a result of the intensive heating. The wood drying model was used here due to the lack of a better model for moisture movement in wood during fires.

The predicted (solid line) and measured rates of mass loss from the dowel agree well during the pyrolysis stage (i.e. the slopes agree well), suggesting that

the Arrhenius model for pyrolysis and its constants are reasonably accurate.

An advantage of this model is that it can be used to predict physical variables, such as the mass of the individual components of the dowel (moisture, gases and wood) or the total gas pressure, which cannot be easily measured in an experiment. Some of these results are presented now.

Figure 7 shows the radial distribution of the total gas pressure inside the fuel element at $\phi = 40°$ for different time intervals as predicted by the model. It is seen that the value of the total gas pressure inside the dowel can reach over two atmospheres. Some of the reasons that may cause the rise of the total gas pressure are the temperature increase and the amount
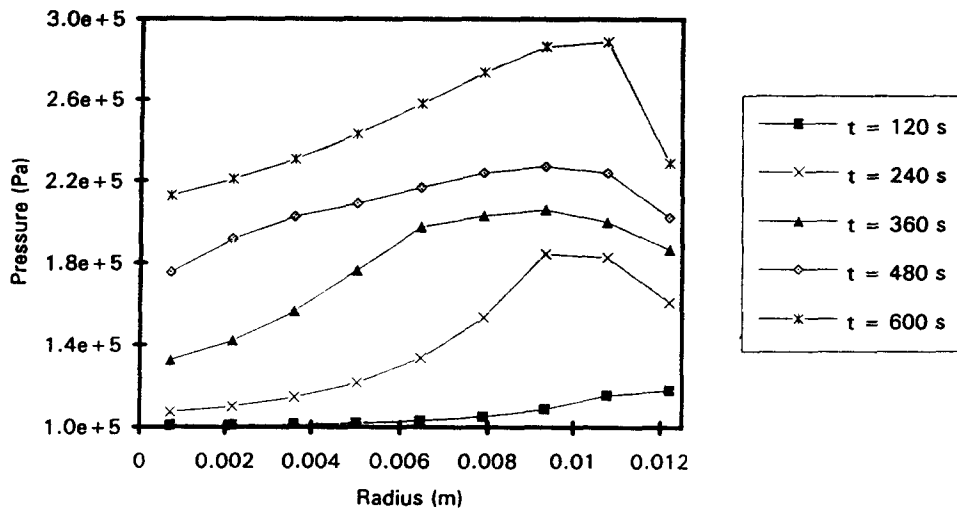
Fig. 7. Radial distribution of gas total pressure at $\phi = 40°$.
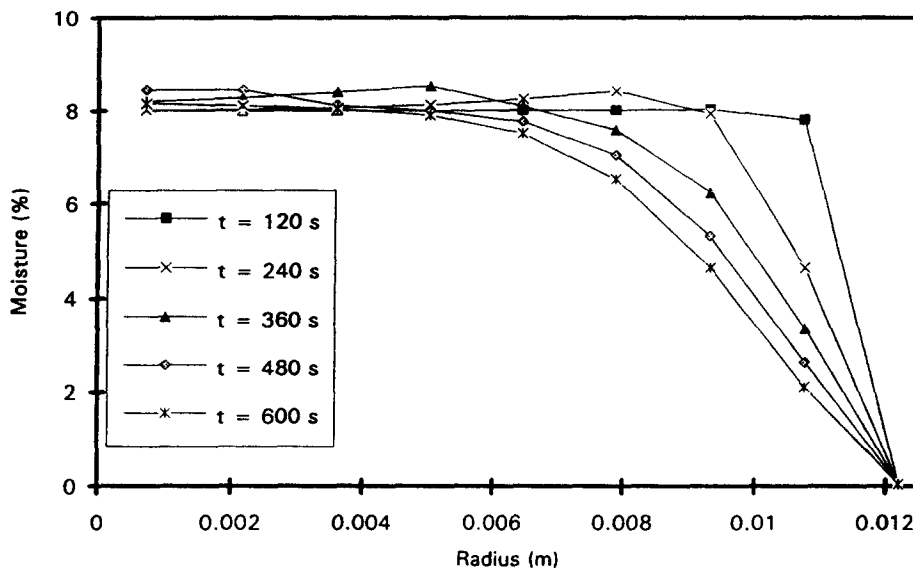
Fig. 8. Radial distribution of moisture content at $\phi = 40°$.

of gases present inside the dowel. The amount of gases present inside the dowel increases when pyrolysis starts. Most of these gases remain trapped inside the dowel causing the total gas pressure to increase. In fires, this pressure rise is relieved by cracking the structure of the wood. The cracks in the structure allow the gases to flow through the wood easily. The model does not account for this cracking phenomenon.

Figure 8 shows the radial distribution of the moisture content of the dowel at $\phi = 40°$ for different time intervals. It is noticed that for locations (inside the dowel) close to the surface, the moisture content decreases monotonically, while for locations further inside, the moisture content increases at first and then decreases later on. As seen in equation (3), the moisture inside the dowel moves from one location to another because of the temperature and moisture gradients. The temperature and moisture gradients

are in opposite directions. In the early stages, the movement of moisture is mainly outward, due to the moisture gradient, because the temperature gradient is still small. As time progresses the temperature gradient increases, creating an inward flow of moisture (from near the surface to further inside). This results in an increased moisture gradient which later on causes the moisture to flow outward again.

SUMMARY

A theoretical model has been developed to study the problem of heat and mass transfer in wooden dowels prior to ignition. The model shows good agreement with the results of the experiments conducted in predicting the temperature history, but the mass loss is not as accurately predicted. The mass loss of wood during the early stage of heating is mainly due to

drying. The drying model did not predict correctly the moisture migration from wood, because it is not designed to accommodate rapid heating of the wood. The mass loss of wood during the later stages of heating is due to pyrolysis of wood. The pyrolysis model predicts accurately the rate of mass loss of wood during the late stages of heating.

The model can be used as a tool in predicting the moisture distribution, temperature distribution, time to ignition and mass loss of each individual component of the dowel.

In general, the model is considered to be a good tool for simulating the processes of heat and mass transfer in wood during fires. Further work needs to be done to improve the drying model.

REFERENCES

1. G. L. Comstock, Directional permeability of softwoods, *Wood Fiber* **1**, 283–289 (1970).
2. O. A. Plumb, G. A. Spolek and B. A. Olmstead, Heat and mass transfer in wood during drying, *Int. J. Heat Mass Transfer* **28**, 1669–1678 (1985).
3. G. Spolek and O. Plumb, Capillary pressure in softwoods, *Wood Sci. Tech.* **15**, 189–199 (1981).
4. A. Kanury, Ignition of cellulosic solids. A review, *Fire Abstracts Rev.* **14**, 24–52 (1972).
5. A. F. Roberts, A review of kinetic data for the pyrolysis of wood and related substances, *Combust. Flame* **14**, 261–272 (1970).
6. J. R. Welker, The pyrolysis and ignition of cellulosic materials. A literature review, *J. Fire Flammability* **1**, 12–29 (1970).
7. C. K. Lee, R. F. Chaiken and J. M. Singer, Charring pyrolysis of wood, *16th International Symposium on Combustion*, pp. 1459–1470 (1976).
8. K. Akita, Studies on the mechanism of ignition of wood, Report on Fire Research no. 9, 1, 51, 77, 99, Institute of Japan (1959).
9. P. Klason, Theory of the dry distillation of wood, *I. J. Prakt. Chem.* **90**, 413 (1914).
10. R. M. J. Nelson, Diffusion of bound water in wood. Part 2. A model for isothermal diffusion, *Wood Sci. Tech.* **20**, 235–251 (1986a).
11. R. M. J. Nelson, Diffusion of bound water in wood. Part

3. A model for nonisothermal diffusion, *Wood Sci. Tech.* **20**, 309–328 (1986b).
12. J. F. Siau, *Flow in Wood*. Springer, New York (1986).
13. C. Moyne, Contribution a l'etude du transfert simultane de chaleur et de masse lors du sechage sous vide d'un bois resineux, Ph.D. Thesis, Nancy University, France (1982).
14. H. Kung, The burning of vertical wooden slabs, *15th International Symposium on Combustion*, pp. 243–253 (1974).
15. B. Fredlund, A model for heat and mass transfer in timber structures during fire. A theoretical, numerical and experimental study, Ph.D. Thesis, Lund University, Sweden (1988).
16. E. J. Kansa, H. E. Perlee and R. F. Chaiken, Mathematical model of wood pyrolysis including internal forced convection, *Combustion and Flame*, **29**, 311–324 (1977).
17. P. Shusheng, R. B. Keey and T. A. G. Langrish, Modeling the temperature profiles within boards during the high-temperature drying of pinus radiata timber: the influence of airflow reversals, *Int. J. Heat Mass Transfer* **38**, 189–205 (1995).
18. C. T. Kiranoudis, Z. B. Maroulis and D. Marinos-Kouris, Heat and mass transfer model building in drying with multiresponse data, *Int. J. Heat Mass Transfer* **38**, 463–480 (1995).
19. S. Whitaker, Heat and mass transfer in granular porous media, In *Advances in Drying*. Hemisphere, Washington (1978).
20. K. M. Krall, Local heat transfer around a transverse circular cylinder, Ph.D. Thesis, University of Minnesota (1969).
21. A. F. Mills, *Heat and Mass Transfer*. Irwin, Chicago, Illinois (1995).
22. J. A. Mardini, Heat and mass transfer in wood prior to ignition in fires, Ph.D. Thesis, University of California, Los Angeles (1993).
23. A. J. Stamm, *Wood and Cellulose Science*. Ronald Press, New York (1964).
24. C. Skaar and J. F. Siau, Thermal diffusion of bound water in wood, *Wood Sci. Tech.* **15**, 105–112 (1981).
25. R. Siegel and J. R. Howell, *Thermal Radiation Heat Transfer* (2nd Edn). McGraw-Hill, New York (1981).
26. R. Sussot, Characterization of the thermal properties of forest fuels by combustible gas analysis, *Forest Sci.* **28**, 404–420 (1982).
27. S. Patankar, *Numerical Heat Transfer and Fluid Flow*. Hemisphere, Washington DC (1982).
28. A. TenWolde, J. D. McNatt and L. Krahn, Thermal properties of wood and wood panel products for use in buildings—Part of the National Program for Building thermal envelope systems and materials, Forest Products Laboratory, Madison, Wisconsin, September (1988).